Molecular Crystals and Liquid Crystals

Publication details, including instructions for authors and subscription information:
http://www.tandfonline.com/loi/gmcl20

Nanostructure Control by Interlaminated Fullerene/Phthalocyanine Ultrathin Films in p-i-n Organic Solar Cells

Hiroki Shiokawa [a] & Masahiro Hiramoto [a]

[a] Material and Life Science, Graduate School of Engineering, Osaka University, Suita, Osaka, Japan

Version of record first published: 22 Sep 2010

To cite this article: Hiroki Shiokawa & Masahiro Hiramoto (2008): Nanostructure Control by Interlaminated Fullerene/Phthalocyanine Ultrathin Films in p-i-n Organic Solar Cells, Molecular Crystals and Liquid Crystals, 491:1, 277-283

To link to this article: http://dx.doi.org/10.1080/15421400802330945

Mol. Cryst. Liq. Cryst., Vol. 491, pp. 277–283, 2008

ISSN: 1542-1406 print/1563-5287 online
DOI: 10.1080/15421400802330945

Taylor & Francis
Taylor & Francis Group

Nanostructure Control by Interlaminated Fullerene/Phthalocyanine Ultrathin Films in *p-i-n* Organic Solar Cells

Hiroki Shiokawa and Masahiro Hiramoto
Material and Life Science, Graduate School of Engineering, Osaka University, Suita, Osaka, Japan

The concept of ultrathin-film interlamination was demonstrated to be effective for nanostructure control of i-layer of the p-i-n organic solar cells. Crystalline phthalocyanine-amorphous fullerene nanocomposite structure, in which the photogenerated electrons and holes can transport to respective electrodes through spatially separated routes, could be intentionally fabricated. p-i-n cells incorporating interlaminated i-layer showed 1.3% solar energy conversion efficiency.

Keywords: crystalline-amorphous nanocomposite; fullerene; nanostructure control; organic *p-i-n* solar cells; percolation; ultra-thin film interlamination

INTRODUCTION

We previously reported *p-i-n* junction organic solar cells [1–3]. *I*-interlayers of *p-i-n* cells were composed of the codeposited layer of *n*-type and *p*-type organic semiconductors acting as acceptors and donors and photocarrier generation occurs at their molecular contact sites. In order to extract photogenerated electrons and holes to respective electrodes efficiently, spatially separated routes should be formed in the codeposited layer, namely, nanostructure of codeposited *i*-interlayer should be controlled intentionally. Based on the results using organic vertical superlattice [4], nanostructure control reaching 10 nm should be necessary.

As a new method for nanostructure control, in this study, we decided to develop the ultrathin-film interlamination method. Figure 1 shows

Address correspondence to Masahiro Hiramoto, Material and Life Science, Graduate School of Engineering, Osaka University Yamadaoka, Suita, Osaka 565-0871, Japan. E-mail: hiramoto@chem.eng.osaka-u.ac.jp

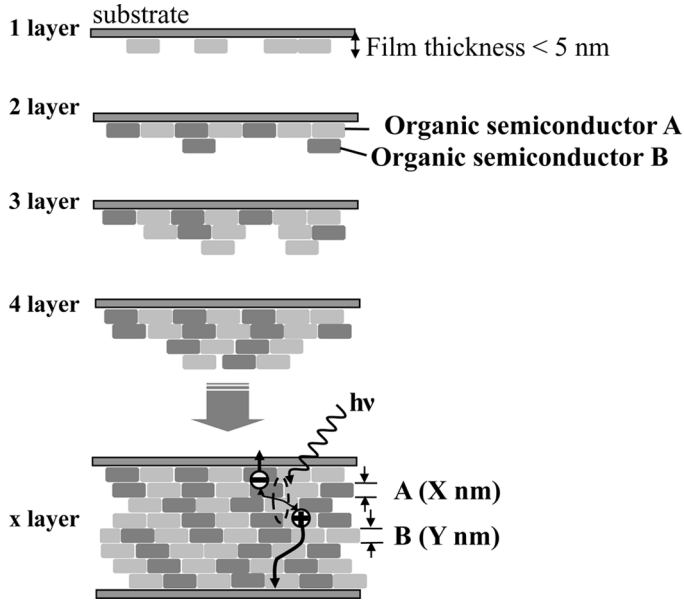

FIGURE 1 Concept of ultrathin-film interlamination.

the concept of the ultrathin-film interlamination. Organic ultrathin-films of the thickness less than 5 nm do not form perfect uniform plane but form island structure. When such ultrathin-films of organic semiconductor A and B are alternately deposited, same kinds of semiconductor molecules are expected to cohere easily and each semiconductor molecules is connected by percolation. As a result, the spatially separated transit route for electrons and holes can be ensured. Parameters to control such percolation process are (i) ultrathin-film thickness of semiconductor A (X) and B (Y), (ii) film thickness ratio (X/Y), and (iii) substrate temperature. In this study, we used fullerene (C_{60}) and metal-free phthalocyanine (H_2Pc) as semiconductors A and B, respectively.

Here, we report the *p-i-n* organic solar cells in which the nanostructure of *i*-interlayer is controlled by ultrathin-film interlamination method. Photo-electric conversion efficiency of 1.3% was observed.

EXPERIMENTAL

Cell structure is shown in Figure 2. H_2Pc as a *p*-type layer, interlaminated layer as an *i*-layer, and naphthalene derivative (NTCDA) as an

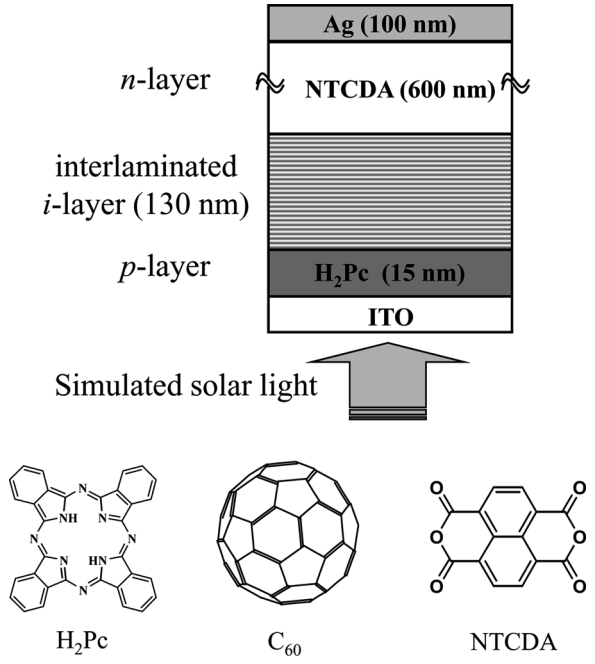

FIGURE 2 Structure of *p-i-n* cell incorporating interlaminated *i*-layer.

n-layer were successively deposited by vacuum evaporation at 1×10^{-3} Pa onto indium tin oxide (ITO) glass substrates at room temperature. Total thickness of interlaminated *i*-layer was 130 nm. Ultrathin-film thickness per 1 layer was changed from 5 to 1 nm. The alternate deposition of C_{60} and H_2Pc was performed by using the shutters above respective sources. To prevent the electrical shorting of cells, 600 nm-thick NTCDA film was used as *n*-layer [5,6]. The current-voltage (J-V) characteristics were measured at a pressure of 10^{-1} Pa under irradiation of AM 1.5 simulated solar light.

RESULTS AND DISCUSSION

As a first step, we decreased the thickness of ultrathin-film from 5 to 1 nm while keeping C_{60} thickness (X) and H_2Pc thickness (Y) equal (X = Y). Figure 3 shows the dependence of the short-circuit photocurrent density (J_{sc}) on the ultrathin-film thickness (X = Y). J_{sc} showed small value of about 1 mAcm^{-2} from 5 to 4 nm. However, it revealed

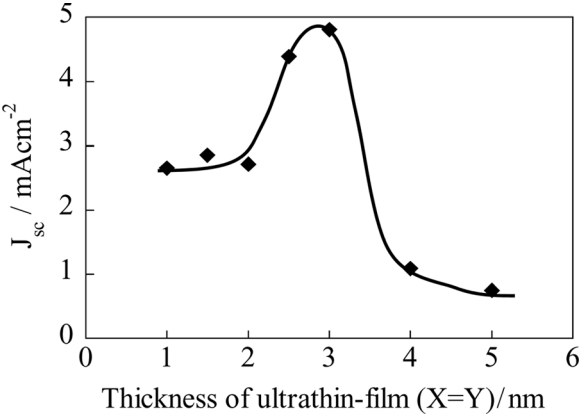

FIGURE 3 Dependence of the short-circuit photocurrent density (J_{sc}) on the ultrathin-film thickness (X = Y) in interlaminated *i*-layer of *p-i-n* cell. C_{60} thickness (X) and H_2Pc thickness (Y) were kept equal (X = Y).

to increase rapidly below 4 nm and reached maximum from 3 to 2.5 nm. This result strongly suggests that above 4 nm each ultrathin films have uniform plane and below 3 nm each ultrathin films do not have perfect plane and have island structure. We concluded that below 3 nm percolation process shown in Figure 1 took place.

We optimized X and Y values while keeping their sum (X + Y) to be 5 or 6 nm. Total thickness of interlaminated *i*-layer was always kept to 130 nm. Typical current-voltage (J-V) characteristics are shown in Figure 4. In the case of X + Y = 5 nm, J-V curve showing fairly large fill factor (FF) of 0.52 was observed for X = Y = 2.5 nm (curve A). In the case of X + Y = 6 nm, J-V curve showing considerable large J_{sc} of 6.3 $mAcm^{-2}$ was observed for the combination of X = 3.5 nm and Y = 2.5 nm (curve B). For comparison, J-V curve for *p-i-n* cell incorporating C_{60}:H_2Pc (1:1) codeposited *i*-layer of the thickness of 130 nm is shown (curve C). C_{60}:H_2Pc layer codeposited at room temperature had been proved to be molecular mixing [7]. Superior characteristics of the interlaminated *i*-layer compared to that of thecodeposited *i*-layer strongly suggest that spatially separated routes for photogenerated electrons and holes are formed by the present ultrathin-film interlamination method.

Figure 5(a) shows the SEM image of cross section of interlaminated *i*-layer (X = Y = 2.5 nm). A lot of small crystals having size of around 100 nm were surrounded by smooth parts (see Fig. 5(b)). In addition,

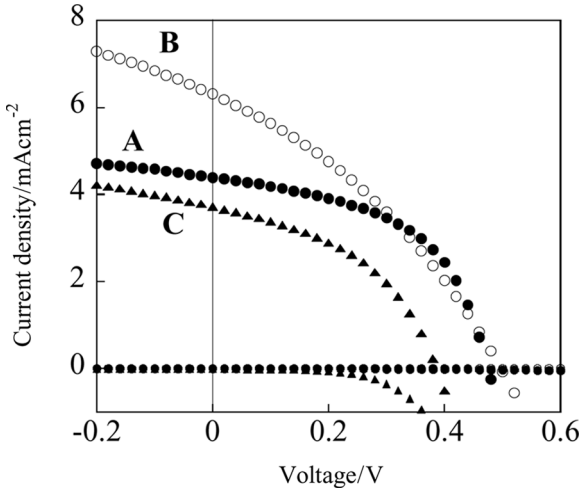

FIGURE 4 Current–voltage (J-V) curves for *p-i-n* cells incorporating interlaminated *i*-layers of the composition of X = Y = 2.5 nm (curve A) and of X = 3.5 nm/Y = 2.5 nm (curve B). J-V curve for *p-i-n* cell incorporating C_{60}:H_2Pc (1:1) codeposited *i*-layer is also shown (curve C). Total *i*-layer thicknesses for all cells were same (130 nm). Cell parameters; J_{sc}:4.4 mAcm^{-2}, V_{oc}:0.48 V, FF:0.52, Efficiency:1.3% (curve A); J_{sc}:6.3 mAcm^{-2}, V_{oc}:0.5 V, FF:0.34, Efficiency:1.2% (curve B); J_{sc}:3.7 mAcm^{-2}, V_{oc}:0.39 V, FF:0.44, Efficiency:0.74% (curve C). Light Intensity transmitted through ITO substrate was 85.8 mWcm^{-2}.

this film showed X-ray diffraction peak attributed to H_2Pc and no peak attributed to C_{60}. Thus, we concluded that the crystalline H_2Pc was surrounded by amorphous C_{60}. In this crystalline H_2Pc-amorphous C_{60} nano-composite structure, electrons and holes photogenerated at C_{60}/H_2Pc interface can transport to respective electrodes through spatially separated routes. As a result, photocurrent generation was enhanced compared to the codeposited film having no spatially separated routes in the molecular mixture.

For X = Y = 2.5 nm, maximum J_{sc} value (6.5 mAcm^{-2}) was observed at the total thickness of laminated *i*-layer of 70 nm. Above 70 nm, J_{sc} value decreased rapidly. Resistance of laminated layer is inevitably increased for thicker laminated layer. For further improvement of cell performance, we are now performing the further optimization of nanostructure of *i*-layer by controlling the substrate temperature during alternating deposition.

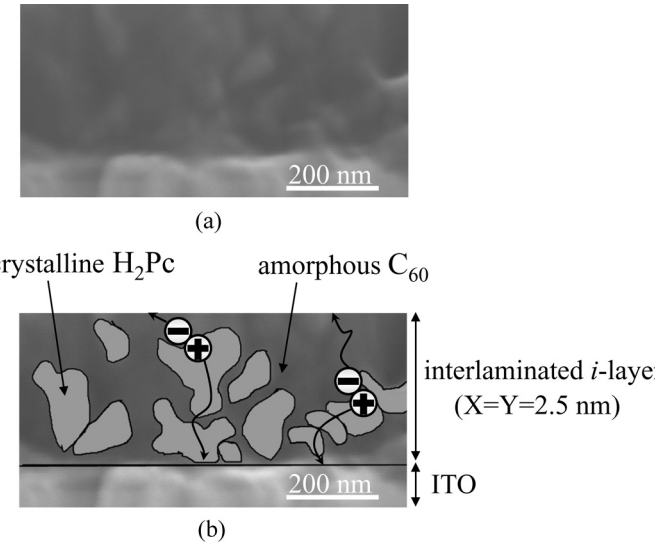

FIGURE 5 (a) SEM image of cross section of interlaminated *i*-layer ($X = Y = 2.5$ nm). (b) Crystalline H_2Pc parts of Figure 5(a) are traced. In crystalline H_2Pc-amorphous C_{60} nano-composite structure, electrons and holes photogenerated at C_{60}/H_2Pc interface can transport to respective electrodes through spatially separated routes.

CONCLUSION

We successfully demonstrated the concept of ultrathin-film interlamination to make crystalline H_2Pc-amorphous C_{60} nano-composite structure. In this nanostructure, electrons and holes photogenerated at C_{60}/H_2Pc interface can transport to respective electrodes through spatially separated routes. Organic *p-i-n* cells incorporating interlaminated *i*-layer showed the photo-electric conversion efficiency of 1.3%. Larger conversion efficiency would be possible by optimizing the substrate temperature.

REFERENCES

[1] Hiramoto, M., Fujiwara, H., & Yokoyama, M. (1991). *Appl. Phys. Lett.*, *58*, 1062.
[2] Hiramoto, M., Fujiwara, H., & Yokoyama, M. (1992). *J. Appl. Phys.*, *72*, 3781.
[3] Suemori, K., Miyata, T., Yokoyama, M., & Hiramoto, M. (2005). *Appl. Phys. Lett.*, *86*, 063509.
[4] Hiramoto, M., Yamaga, T., Danno, M., Suemori, K., Matsumura, Y., & Yokoyama, M. (2006). *Appl. Phys. Lett.*, *88*, 213105.

[5] Suemori, K., Miyata, T., Yokoyama, M., & Hiramoto, M. (2004). *Appl. Phys. Lett.*, *85*, 6269.
[6] Surmori, K., Matsumura, Y., Yokoyama, M., & Hiramoto, M. (2006). *Jpn. J. Appl. Phys.*, *45*, L472.
[7] Suemori, K., Miyata, T., Hiramoto, M., & Yokoyama, M. (2004). *Jpn. J. Appl. Phys.*, *43*, L1014.